

Ecosystem functional response across precipitation extremes in a sagebrush steppe

Andrew T. Tredennick¹, Andrew R. Kleinhesselink², Bret Taylor³, and Peter B. Adler¹

¹Department of Wildland Resources and the Ecology Center, Utah State University, Logan, Utah 84322

²Department of Ecology and Evolutionary Biology, University of California, Los Angeles, Los Angeles, California 90095

³United States Department of Agriculture, Agriculture Research Station, U.S. Sheep Experiment Station, Dubois, Idaho 83423

Corresponding author:
Andrew T. Tredennick¹

Email address: atredenn@gmail.com

ABSTRACT

Background. Precipitation is predicted to become more variable in the western United States, meaning years of above and below average precipitation will become more common. Periods of extreme precipitation are major drivers of ecosystem functioning in water limited grasslands, but how ecosystems respond to precipitation may change as the duration of above and below average periods increases. Changes in ecosystem functional response could reflect compensatory changes in species composition or species reaching physiological thresholds at extreme precipitation levels.

Methods. We conducted a five year precipitation manipulation experiment in a sagebrush steppe ecosystem in Idaho, United States. We used drought and irrigation treatments (approximately 50% decrease/increase) to investigate whether ecosystem functional response remains consistent at extreme precipitation levels. We recorded data on aboveground net primary productivity (ANPP), species abundance, and soil moisture. We fit a generalized linear mixed effects model to determine if the relationship between ANPP and soil moisture differed among treatments. We used nonmetric multidimensional scaling to quantify community composition over the five years.

Results. Ecosystem functional response, defined as the relationship between soil moisture and ANPP was similar among drought and control treatments, but the irrigation treatment had a lower slope than the control treatment. However, ANPP response to available soil moisture was weak and uncertain regardless of treatment, with all slopes overlapping zero. There was also large variation in ANPP within-years. Plant community composition was remarkably stable over the course of the experiment and did not differ among treatments.

Discussion. Despite some evidence that ecosystem functional response was less positive under extreme wet conditions, the response of ANPP to soil moisture was consistently weak and community composition was remarkably stable. Ecosystem functional responses across treatments was not related to compensatory shifts at the plant community level, but instead reflects the weak and variable responses of individual species. Such responses may be due to bet hedging strategies where species respond weakly to even extreme levels of soil moisture to ensure low variance of long-term success.

1 INTRODUCTION

The functional response of aboveground net primary productivity (ANPP) to water availability (e.g., soil moisture) can be characterized by fitting a model to historical observations of ANPP and soil moisture at a given site. However, the fitted functional response may provide an incomplete picture because future conditions are likely to be outside the historical range of variability (Smith, 2011). For example, historical

46 trends may underestimate the potential for the soil moisture-ANPP relationship to saturate or weaken if
47 soil moisture is pushed far beyond typical levels. Saturating relationships are actually common (Hsu et al.,
48 2012; Gherardi and Sala, 2015b), perhaps because other resources, like nitrogen, become more limiting
49 in wet years than dry years. Knowing the curvature of the soil moisture-ANPP relationship at extreme
50 precipitation levels is critical for understanding how ecosystems will respond to chronic alterations in
51 water availability.

52 Another problem with relying on historical ecosystem functional responses is that they are not static.
53 Changes in species identities and abundances can alter an ecosystem's functional response to water
54 availability because different species have different physiological thresholds for producing biomass.
55 Smith et al. (2009) introduced the 'Hierarchical Response Framework' for understanding the interplay of
56 community composition and ecosystem functioning in response to resource manipulations over time. In
57 the near term, ecosystem functioning such as ANPP will reflect the physiological responses of individual
58 species to the manipulated resource level. For example, ANPP may decline under simulated drought
59 because the initial community consisted of drought-intolerant species (Hoover et al., 2014). Ecosystem
60 functioning may recover over longer time spans as new species colonize or initial species reorder in
61 relative abundance. For example, ANPP may initially decline, but eventually rise back to pre-treatment
62 levels once drought-tolerant species become more abundant and compensate for drought-intolerant species
63 (Hoover et al., 2014). It is also possible that ecosystem functioning shifts to a new mean state, reflecting
64 the suite of species in the new community (Knapp et al., 2012).

65 Manipulating potentially limiting resources, like precipitation, offers a route to understanding how
66 ecosystems will respond to resource levels that fall outside the historical range of variability (Avolio et al.,
67 2015; Gherardi and Sala, 2015a; Knapp et al., 2017). Altering the amount of precipitation over many
68 years should provide insight into the time scales at which water-limited ecosystems respond to chronic
69 resource alteration. We propose four alternative predictions for the effect of precipitation manipulation
70 on the ecosystem functional response to soil moisture based on the Hierarchical Response Framework
71 (Fig. 1). We define 'ecosystem functional response' as the relationship between available soil moisture
72 and ANPP. The four predictions are based on possible outcomes at the community (e.g., community
73 composition) and ecosystem (e.g., soil moisture-ANPP regression) levels.

74 First, altered precipitation changes neither ecosystem functional response nor community composition
75 (Fig. 1, top left). In this case, changes in ANPP simply follow the soil moisture-ANPP relationship under
76 ambient conditions. This corresponds to the early phases of the Hierarchical Response Framework, where
77 ecosystem response follows the physiological responses of individual species. Second, the ecosystem
78 functional response changes but community composition remains the same (Fig. 1, top right). A saturating
79 soil moisture-ANPP response fits this scenario, where individual species hit physiological thresholds or
80 are limited by some other resource. Third, the ecosystem functional response is consistent but underlying
81 community composition changes (Fig. 1, bottom left). In this case, changes in species' identities or
82 abundances occur in response to altered precipitation levels and species more suited to the new conditions
83 compensate for reduced function of initial species. Fourth, and last, both ecosystem functional response
84 and community composition change (Fig. 1, bottom right). New species, or newly abundant species, with
85 different physiological responses completely reshape the ecosystem functional response.

86 All four outcomes are possible in any given ecosystem, but the time scales at which the different
87 scenarios play out likely differ (Smith et al., 2009; Wilcox et al., 2016; Knapp et al., 2017). Thus, our task
88 is not to test the validity of the Hierarchical Response Framework, but rather to amass information on
89 how quickly ecosystem functional responses change in different ecosystems. We also need to understand
90 whether changes at the ecosystem level are driven by community level changes or individual level
91 responses.

92 To that end, here we report the results of a five-year precipitation manipulation experiment in a
93 sagebrush steppe grassland. We imposed drought and irrigation treatments (approximately $\pm 50\%$) and
94 measured ecosystem (ANPP) and community (species composition) responses. We focus on how the
95 drought and irrigation treatments affect the relationship between available soil moisture and ANPP, and if
96 community dynamics underlie the ecosystem responses. In particular, we are interested in the consistency
97 of the soil moisture-ANPP relationship among treatments. Is the relationship steeper under the drought
98 treatment, at low soil moisture? Does the relationship saturate under the irrigation treatment, at high soil
99 moisture? To answer these questions we fit a generalized linear mixed effects model to test whether the
100 regressions differed among treatments. We also analyzed community composition over time, allowing us

101 to place our experimental results within the framework our competing predictions (Fig. 1).

102 2 METHODS

103 2.1 Study Area

104 We conducted our precipitation manipulation experiment in a sagebrush steppe community at the United
105 States Sheep Experimental Station (USSES) near Dubois, Idaho (44.2° N, 112.1° W), 1500 m above
106 sea level. The plant community is dominated by the shrub *Artemisia tripartita* and three perennial
107 bunchgrasses, *Pseudoroegneria spicata*, *Poa secunda*, and *Hesperostipa comata*. During the period of our
108 experiment (2011 – 2015), average mean annual precipitation was 265 mm year⁻¹ and mean monthly
109 temperature ranged from -5.2°C in January to 21.8°C in July. Between 1926 and 1932, range scientists
110 at the USSES established 26 permanent 1 m² quadrats to track vegetation change over time. In 2007,
111 we (well, one of us [P. Adler]) relocated 14 of the original quadrats, six of which were inside a large,
112 permanent livestock enclosure. We use these six plots as control plots that have received no treatment,
113 just ambient precipitation, in the experiment described below.

114 2.2 Precipitation Experiment

115 In spring 2011, we (well, two of us [A. Kleinbesselink and P. Adler]) established 16 new 1 m² plots located
116 in the same enclosure as the six control plots. We avoided areas on steep hill slopes, areas with greater
117 than 20% cover of bare rock, and areas with greater than 10% cover of the shrubs *Purshia tridentata*
118 and/or *Amelanchier utahensis*. We established the new plots in pairs and randomly assigned each plot in a
119 pair to receive a “drought” or “irrigation” treatment.

120 Drought and irrigation treatments were designed to decrease and increase the amount of ambient
121 precipitation by 50%. To achieve this, we used a system of rain-out shelters and automatic irrigation
122 (Gherardi and Sala, 2013). The rain-out shelters consisted of transparent acrylic shingles 1-1.5 m above
123 the ground that covered an area of 2.5 × 2 m. The shingles intercepted approximately 50% of incoming
124 rainfall, which was channeled into 75 liter containers. Captured rainfall was then pumped out of the
125 containers and sprayed on to the adjacent irrigation plot via two suspended sprinklers. Pumping was
126 triggered by float switches once water levels reached about 20 liters. We disconnected the irrigation
127 pumps each fall and reconnected them, often with difficulty, each spring. The rain-out shelters remained
128 in place throughout the year.

129 We monitored soil moisture in four of the drought-irrigation pairs using Decagon Devices (Pullman,
130 Washington) 5TM and EC-5 soil moisture sensors. We installed four sensors around the edges of each plot,
131 two at 5 cm soil depth and two at 25 cm soil depth. We also installed four sensors in areas nearby the four
132 selected plot pairs to measure ambient soil moisture at the same depths. Soil moisture measurements were
133 automatically logged every four hours. We coupled this temporally intensive soil moisture sampling with
134 spatially extensive readings taken at six points within all 16 plots and associated ambient measurement
135 areas. These snapshot data were collected on 06-06-2012, 04-29-2015, 05-07-2015, 06-09-2015, and
136 05-10-2016¹ using a handheld EC-5 sensor.

137 Analyzing the response to experimental treatments was complicated by the fact that we did not directly
138 monitor soil moisture in each plot on each day of the experiment. Only a subset of plots were equipped
139 with soil moisture sensors, and within those plots, one or more of the sensors frequently failed to collect
140 data. To remedy these problems, and to produce average daily soil moisture values for the ambient,
141 drought, and irrigation conditions, we used a statistical model to predict the average treatment effects on
142 soil moisture during the course of the experiment.

143 We first averaged the observed soil moisture for each day and within each plot. Then we standardized
144 the averages within each plot group by subtracting the average ambient soil moisture in that plot group
145 and dividing by the standard deviation of the ambient soil moisture in that plot group. We then found the
146 difference between the standardized ambient soil moisture and the standardized drought and irrigation
147 soil moisture within each plot group. These transformations ensured that the treatment effects in each plot
148 were appropriately scaled by the local ambient conditions within each plot group.

¹Dates formatted as: mm-dd-yyyy.

We then modeled the daily deviation from ambient conditions of the drought and irrigation treatments using a linear mixed effects model with independent variables for treatment, season (winter, spring, summer, fall), rainfall, and all two-way interactions. Rainy days were defined as any day in which precipitation was recorded and average temperature was above 3°C. The day immediately following rainfall was also classified as rainy. We fit the model using the `lme4::lmer()` function (Bates et al., 2015) in R (R Core Team, 2016), with random effects for plot group and date. We weighted observations by the number of unique sensors or spot measurements that were taken in each plot on that day. We then used the model to predict the average daily soil moisture in the treated plots based on the average daily ambient soil moisture. We could only predict soil moisture in the treated plots on days for which we took at least one ambient soil moisture measurement.

2.3 Data Collection

We estimated aboveground net primary productivity (ANPP) using a radiometer to relate ground reflectance to plant biomass (see Byrne et al., 2011, for a review). We recorded ground reflectance at four wavelengths, two associated with red reflectance (626 nm and 652 nm) and two associated with near-infrared reflectance (875 nm and 859 nm). At each plot in each year, we took four readings of ground reflectances at the above wavelengths. We also took readings in 12 (2015), 15 (2012, 2013, 2014), or 16 (2016) calibration plots adjacent to the experimental site, in which we harvested all aboveground biomass, dried it to a constant weight at 60°C, and weighed it to estimate ANPP.

For each plot and year, we averaged the four readings for each wavelength and then calculated a greenness index based on the same bands used to calculate NDVI using the MODIS and AVHRR bands for NDVI. We regressed the greenness index against the dry biomass weight from the ten calibration plots to convert the greenness index to ANPP. We fit regressions to a MODIS-based index and an AVHRR-based index for each year and retained the regression with the better fit based on R^2 values. We then predicted ANPP using the best regression equation for each year (Appendix 1).

Species composition data came from two sources: yearly census maps for each plot made using a pantograph (Hill, 1920) and yearly counts of annual species in each plot. We extracted the mapped information to obtain data on the density of all annuals and perennials forbs, the basal cover of perennial grasses, and the canopy cover of shrubs. We made a large plot-treatment-year by species matrix, where columns were filled with either basal cover or density, depending on the measurement made for the particular species. We standardized the values in each column so we could analyze the different types of data together. This puts all abundance values on the same scale, meaning that common and rare species are weighted equally. This approach is anti-conservative for detecting community change if we assume that rare species will respond more than common ones, which biases our approach toward detecting compositional changes.

2.4 Data Analysis

Our main goal was to test whether the relationship between ANPP and soil moisture differed among the drought, control, and irrigation treatments. Based on our own observations and previous work at our study site (Blaisdell, 1958; Dalglish et al., 2011; Adler et al., 2012), we chose to use cumulative volumetric water content from March through June as our metric of soil moisture (hereafter referred to as ‘VWC’). To achieve this goal, we fit a generalized linear mixed effects regression model with $\log(\text{ANPP})$ as the response variable and VWC and treatment as fixed effects. Plot and year of treatment were included as random effects to account for non-independence of observations, as described below. We log-transformed ANPP to account for heteroscedasticity. Both $\log(\text{ANPP})$ and VWC were standardized to have mean 0 and unit variance before fitting the model [i.e., $(x_i - \bar{x})/\sigma_x$].

Our model is defined as follows:

$$\mu_i = \beta \mathbf{x}_i + \gamma_{j(i)} \mathbf{z}_i + \eta_t, \quad (1)$$

$$\mathbf{y} \sim \text{Normal}(\boldsymbol{\mu}, \sigma^2), \quad (2)$$

where μ_i is the deterministic prediction from the regression model for observation i , which is associated with plot j and treatment year t . β is the vector of coefficients for the fixed effects in the design matrix \mathbf{X} . Each row of the design matrix represents a single observation (\mathbf{x}_i) and is a vector with the following

elements: 1 for the intercept, a binary 0 or 1 if the treatment is “drought”, a binary 0 or 1 if the treatment is “irrigation”, the scaled value of VWC, binary “drought” value times VWC, and binary “irrigation” value times VWC. Thus, our model treats “control” observations as the main treatment and then estimates intercept and slope offsets for the “drought” and “irrigation” treatments. In reference to our model, the hypotheses we wish to test are:

H1. The coefficient for drought \times VWC is positive and different from zero.

H2. The coefficient for irrigation \times VWC is negative and different from zero.

We include two random effects to account for the fact that observations within plots and years are not independent. Specifically, we include plot-specific offsets (γ) for the intercept and slope terms and year-specific intercept offsets (η_t). The covariate vector \mathbf{z}_i for each observation i has two elements: a 1 for the intercept and the scaled value of VWC for that plot and year. The plot-specific coefficients are modeled hierarchically, where plot level coefficients are drawn from a multivariate normal distribution with mean 0 and a variance-covariance structure that allows the intercept and slope terms to be correlated:

$$\gamma_{j(i)} \sim \text{MVN}(0, \Sigma), \quad (3)$$

where Σ is the variance-covariance matrix and $j(i)$ reads as “plot j associated with observation i ”. The random year effects (η) are drawn from a normal prior with mean 0 and standard deviation σ_{year} , which was drawn from a half-Cauchy distribution. A full description of our model is in Appendix 2.

We fit the model using a Bayesian approach and obtained posterior estimates of all unknowns via the No-U-Turn Hamiltonian Monte Carlo sampler in Stan (Stan Development Team, 2016b). We used the R package ‘rstan’ (Stan Development Team, 2016a) to link R (R Core Team, 2016) to Stan. We obtained samples from the posterior distribution for all model parameters from four parallel MCMC chains run for 10,000 iterations, saving every 10th sample. Trace plots of all parameters were visually inspected to ensure well-mixed chains and convergence. We also made sure all scale reduction factors (\hat{R} values) were less than 1.1 (Gelman and Hill, 2009).

We used nonmetric multidimensional scaling (NMDS) based on Bray-Curtis distances to see if community composition differed among treatments through time. We first calculated Bray-Curtis distances among all plots for each year of the experiment and then extracted those distances for use in the NMDS. Some values of standardized species’ abundances were negative, which is not allowed for calculating Bray-Curtis distances. We simply added ‘2’ to each abundance value to ensure all values were greater than zero. We plotted the first two axes of NMDS scores to see if community composition overlapped, or not, among treatments in each year. We used the `vegan::metaMDS()` function (Oksanen, 2016) to calculate Bray-Curtis distances and then to run the NMDS analysis. We used the `vegan::adonis()` function (Oksanen, 2016) to perform permutational multivariate analysis of variance to test whether treatment plots formed distinct groupings. To test whether treatment plots were equally dispersed, or not, we used the `vegan::betadisper()` function (Oksanen, 2016).

All R code and data necessary to reproduce our analysis has been archived on Figshare (*link here after acceptance*) and released on GitHub (https://github.com/atredennick/usses_water/releases/v0.1). We also include annotated Stan code in our model description in Appendix 2.

3 RESULTS

Three of our five treatment years fell in years of below average rainfall (Fig. 2A). Thus, those three years represent a lower magnitude of absolute change in precipitation experienced by the treatments. ANPP varied from a minimum of 74.5 g m⁻² in 2014 to a maximum of 237.1 g m⁻² in 2016 when averaged across treatments (Fig. 2C). ANPP was slightly higher in irrigation plots and slightly lower in drought plots (Fig. 2C), corresponding to estimated soil volumetric water content (VWC) differences among treatments (Fig. 2B). Such differences in soil VWC indicate our treatment infrastructure was successful. ANPP was highly variable within years (Fig. 2C).

Cumulative March-June soil moisture had a weak positive effect on ANPP (Table 1; Fig. 3). The effect of soil moisture for each treatment is associated with high uncertainty, however, with 95% Bayesian credible intervals that overlap zero (Table 1). Although the parameter estimates for the effect of soil

moisture overlap zero, the posterior distributions of the slopes all shrank and shifted to more positive values relative to the prior distributions (Fig. A2-2), which indicates the data did influence parameter estimates beyond the information from the uninformative priors. Ecosystem functional response was similar among treatments (Table 1; Fig. 3B), but there is evidence that the slope for the irrigation treatment is less than the slope for the control treatment. This evidence comes from interpreting the posterior distribution of the slope offset for the irrigation treatment, from which we calculate a 99% one-tailed probability that the estimate is less than zero (Fig. 3A, right panel). There was no evidence that the treatment effects became more important over time because there was no directional trend in the random year effects (Fig. A2-3).

Community composition was similar among treatments. In no year did community composition among treatments not overlap, and they were equally dispersed in all years (Table 2; Fig. 5). Community composition was also remarkably stable over time, with no evidence of divergence among treatments (Table 2; Fig. 5).

4 DISCUSSION

Ecosystem response to precipitation extremes depends on the physiological responses of constituent species and the rate at which community composition shifts to favor species better able to take advantage of, or cope with, new resource levels (Smith et al., 2009). Previous work has shown that community compositional shifts can be both rapid, on the order of years (Hoover et al., 2014), and slow, on order of decades (Knapp et al., 2012; Wilcox et al., 2016). Thus, a lingering question is how the time scales of ecosystem response and community change differ among ecosystems, which can be answered by manipulating precipitation to reach extreme levels.

The results of our five year experiment in a sagebrush steppe conform to two of our four predictions, depending on treatment. Neither ecosystem functional response nor community composition changed under chronic drought (Fig. 3A, Fig. 4), consistent with the top left prediction in Fig. 1. Ecosystem functional response under chronic irrigation was different from the control treatment, but community composition remained unchanged (Fig. 3A, Fig. 4), consistent with the top right prediction in Fig. 1. The altered ecosystem functional response under irrigation matched our expectations because we found evidence for a saturating response for the irrigation treatment (Fig. 3A, right panel). However, the response of ANPP to soil moisture in all treatments was consistently weak (Table 1, Fig. A2-2) and within-year variation of ANPP was large (Fig. 3B).

The similarity of ecosystem functional response (Fig. 3) and community composition (Fig. 5) between drought and control treatments is surprising because grasslands generally, and sagebrush steppe specifically, are considered water-limited systems. Indeed, we expected ecosystem functional response, community composition, or both to change under the drought treatment, landing us in any box of Fig. 1 *except* the top left. Why did our drought treatment fail to induce ecosystem or community responses? We can think of three reasons; two are limitations of our study, and one is the life history traits of the species in our focal communities. We first discuss the potential limitations of our study, and then discuss the biological explanation.

First, it could be that our drought manipulation was not large enough to induce a response. That is, a 50% decrease in any given year may not be abnormal given our site's historical range of variability (Knapp et al., 2017). We cannot definitively rule out this possibility, but we have reason to believe our drought treatment *should* have been large enough. Using the methods described by Lemoine et al. (2016), we calculated the percent reduction and increase of mean growing season precipitation necessary to reach the 1% and 99% extremes of the historical precipitation regime at our site (Fig. A3-3). The 1% quantile of precipitation at our site is 110 mm, a 47% reduction from the mean, and the 99% quantile is 414 mm, a 77% increase from mean growing season precipitation (Appendix 3). Thus, our drought treatment represented extreme precipitation amounts, especially in years where ambient precipitation was below average (Fig. 2A). The irrigation treatment may have been too small, yet that is the treatment where we did observe an effect (Fig. 3).

Second, ANPP at our site may be influenced by factors beyond the window of soil moisture (cumulative March-June) we included in our statistical model. For example, temperature can impact ANPP directly (Epstein et al., 1997) and by exacerbating the effects of soil moisture (De Boeck et al., 2011). Measurements of soil moisture likely contain a signal of temperature, through its impact on evaporation

and infiltration, but the measurements will not capture the direct effect of temperature on metabolic and physiological processes. We also did not redistribute snow across our treatments in the winter, and snow melt may spur early spring growth. These statistical issues of missing potentially important covariates could explain the within-year spread of ANPP (Fig 2C, Fig. 3B) and the resulting uncertain relationship we observed between soil moisture and ANPP across all treatments (Table 1, Fig. A2-2).

Third, the life history traits of the dominant species in our study ecosystem may explain the consistently positive, but weak and uncertain, effect of soil moisture on ANPP (Fig. 3). Species that live in variable environments, such as cold deserts, must have strategies to ensure long-term success as conditions vary. One strategy is bet hedging, where species forego short-term gains to reduce the variance of long-term success (Seger, 1987). In other words, species do the same thing every year, with only minimal response to environmental conditions. The dry and variable environment of the sagebrush steppe has likely selected for bet hedging species that can maintain function at low water availability and have weak responses to high water availability. In so doing, the dominant species in our ecosystem avoid “boom and bust” cycles, which corresponds to the weak effect of soil moisture on ANPP (i.e., the Bayesian credible intervals for the slopes in β in Eq. 1 overlapping zero).

Another strategy to deal with variable environmental conditions is avoidance, which would also result in a consistent ecosystem functional response between drought and control treatments. The perennial plants in this cold desert ecosystem are tolerant to drought conditions (Bazzaz, 1979; Franks, 2011, A.R. Kleinhesselink, unpublished data). For example, many of the perennial grasses in our focal ecosystem avoid drought stress by growing early in the growing season (Blaisdell, 1958, A.R. Kleinhesselink, personal observation). Furthermore, the dominant shrub in our focal ecosystem, *Artemisia tripartita*, has access to water deep in the soil profile thanks to a deep root system (Kulmatiski et al., 2017).

The weaker soil moisture-ANPP relationship we observed for the irrigation treatment, evidenced by the less positive slope relative to controls (Fig. 3A, right panel), has three non-exclusive explanations. First, species’ biomass production may have hit physiological thresholds and/or become limited by other factors, such as nitrogen availability (LeBauer and Treseder, 2008). **PETER: DO WE KNOW ANYTHING ABOUT NITROGEN AT USSES? WANT TO ADD A SENTENCE HERE ABOUT HOW LIKELY OR UNLIKEL THIS IS...** Second, the less positive slope could be another indicator of bet hedging in this community. Avoiding high biomass and seed production in wet years could benefit species in the long run if climate conditions are variable. Third, the less positive slope may be a statistical artifact due the variability of ANPP within years and our low sample size.

In conclusion, our results suggest the species in our focal plant community are tolerant of drought conditions and bet hedgers in wet conditions. Longer time series of chronic precipitation alteration may reveal plant community shifts that we did not observe (e.g., Wilcox et al., 2016), in which case species that do not bet hedge may gain prominence and dominate the ecosystem functional response. Our results suggest compositional shifts would have the largest impact at high rainfall because the current community maintained consistent ecosystem functional response at very low water availability.

5 ACKNOWLEDGEMENTS

We thank the many summer research technicians who collected the data reported in this paper and the US Experimental Sheep Station for facilitating work on their property. We also thank Susan Durham for clarifying our thinking on the statistical analyses and Kevin Wilcox for helpful discussions on analyzing community composition data.

6 FUNDING

This research was supported by the Utah Agricultural Experiment Station, Utah State University, and approved as journal paper number XXXX. The research was also supported by the National Science Foundation, through a Postdoctoral Research Fellowship in Biology and Mathematics to ATT (DBI-1400370), a Graduate Research Fellowship to ARK, and grants DEB-1353078 and DEB-1054040 to PBA.

346 7 AUTHOR CONTRIBUTIONS

- 347 • Andrew T. Tredennick collected data, analyzed the data, wrote the paper, prepared figures and/or
348 tables, reviewed drafts of the paper.
- 349 • Andrew R. Kleinhesselink conceived and designed the experiments, performed the experiments,
350 collected data, analyzed the data, reviewed drafts of the paper.
- 351 • Bret Taylor contributed reagents/materials/analysis tools, reviewed drafts of the paper.
- 352 • Peter B. Adler conceived and designed the experiments, performed the experiments, collected data,
353 analyzed the data, reviewed drafts of the paper.

354 8 SUPPLEMENTAL INFORMATION

- 355 **Appendix 1.** Additional methods and information on estimating aboveground net primary productivity.
- 356 **Appendix 2.** Details of the hierarchical Bayesian model, Fig. A2-1, Fig. A2-2, and Fig. A2-3.
- 357 **Appendix 3.** Details on analysis of precipitation historical range of variability and Fig. A3-1.

9 TABLES

Table 1. Summary statistics from the posterior distributions of coefficients for each treatment.

Coefficient	Treatment	Posterior Mean	Posterior Median	Lower 95% BCI	Upper 95% BCI
Intercept	Control	0.22	0.16	-1.25	2.16
Intercept	Drought	0.64	0.44	-1.37	3.79
Intercept	Irrigation	-0.51	-0.37	-2.99	1.26
Slope	Control	1.31	1.14	-0.30	3.83
Slope	Drought	1.18	1.00	-0.62	4.12
Slope	Irrigation	0.83	0.68	-0.61	3.12

Table 2. Results from statistical tests for clustering and dispersion of community composition among precipitation treatments. ‘adonis’ tests whether treatments form unique clusters in multidimensional space; ‘betadisper’ tests whether treatments have similar dispersion. For both tests, P values greater than 0.05 indicate there is no support that the treatments differ.

Year	Test	n	d.f.	F	P
2011	adonis	21	2	1.02	0.42
2011	betadisper	21	2	2.23	0.14
2012	adonis	22	2	1.10	0.34
2012	betadisper	22	2	0.21	0.81
2013	adonis	22	2	1.23	0.14
2013	betadisper	22	2	0.28	0.76
2014	adonis	22	2	0.95	0.54
2014	betadisper	22	2	0.35	0.71
2015	adonis	21	2	1.05	0.40
2015	betadisper	21	2	3.01	0.07
2016	adonis	21	2	1.07	0.33
2016	betadisper	21	2	0.50	0.62

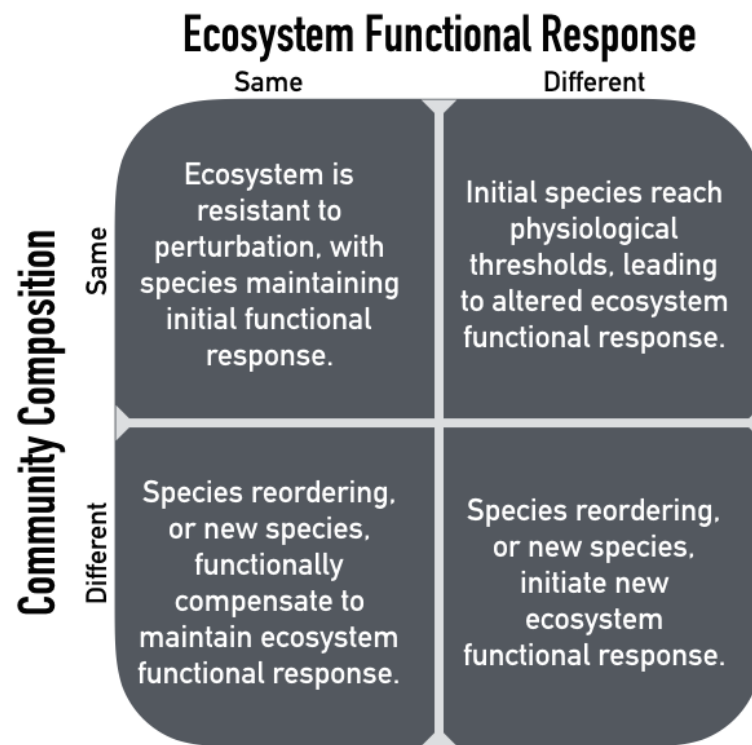


Figure 1. Possible outcomes of chronic resource alteration based on the 'Hierarchical Response Framework' (Smith et al. 2009).

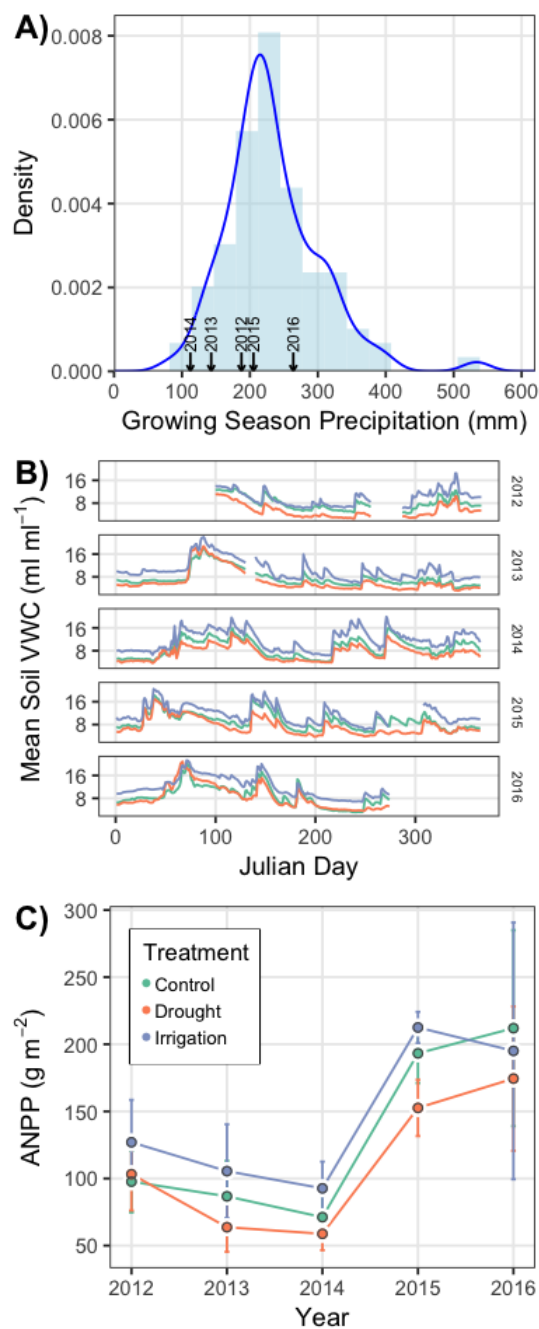


Figure 2. (A) Probability density of historical precipitation from 1926-2016, with the years of the experiment shown with arrows on the x -axis. (B) Observed soil volumetric water content (VWC) over the course of the experiment. (C) Mean (points) ANPP and its standard deviation (error bars) for each year of the experiment.

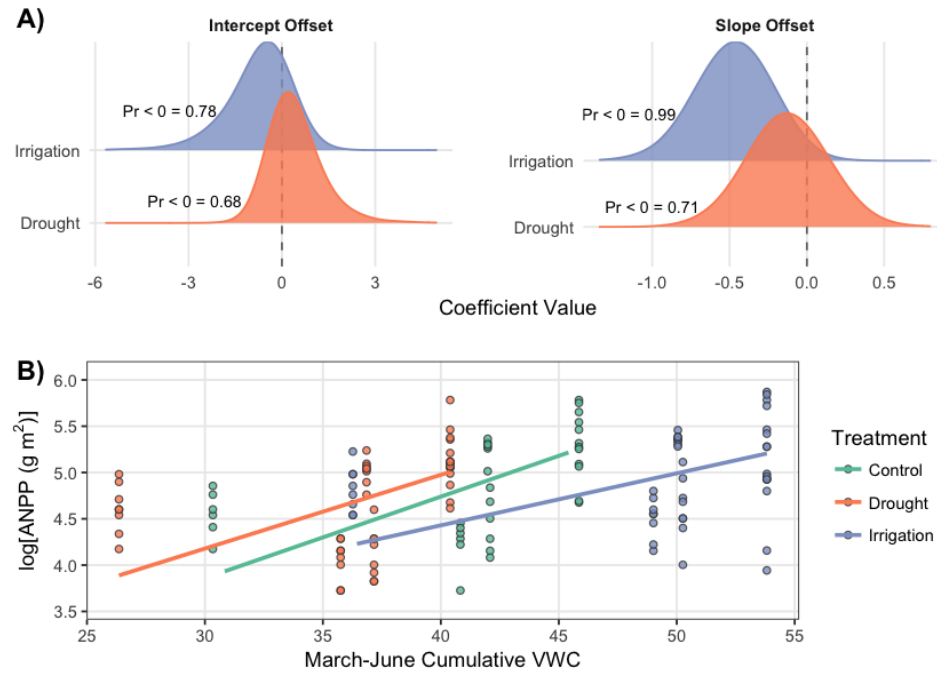


Figure 3. Results from the generalized linear mixed effects model. (A) Posterior distributions of the intercept and slope offsets for the drought and irrigation treatments. Offsets indicate the amount to which the coefficients for drought or irrigation treatments differ from the control treatment estimates. Probabilities (“ $Pr < 0 =$ ”) for each distribution indicate the probability that coefficient is less than zero. Probabilities greater than 0.95 indicate strong support for the coefficient being less than zero. We only show the one-tailed probability for the value being less than zero because the median of each distribution is less than zero. Kernel bandwidths of posterior densities were adjusted by a factor of 5 to smooth the distribution for visual clarity. (B) Scatterplot of the data and model estimates shown as solid lines. Model estimates come from treatment level coefficients (colored lines). Note that we show $\log[ANPP]$ on the y-axis of panel B; this same plot can be seen on the arithmetic scale in supporting material Fig. A2-1.

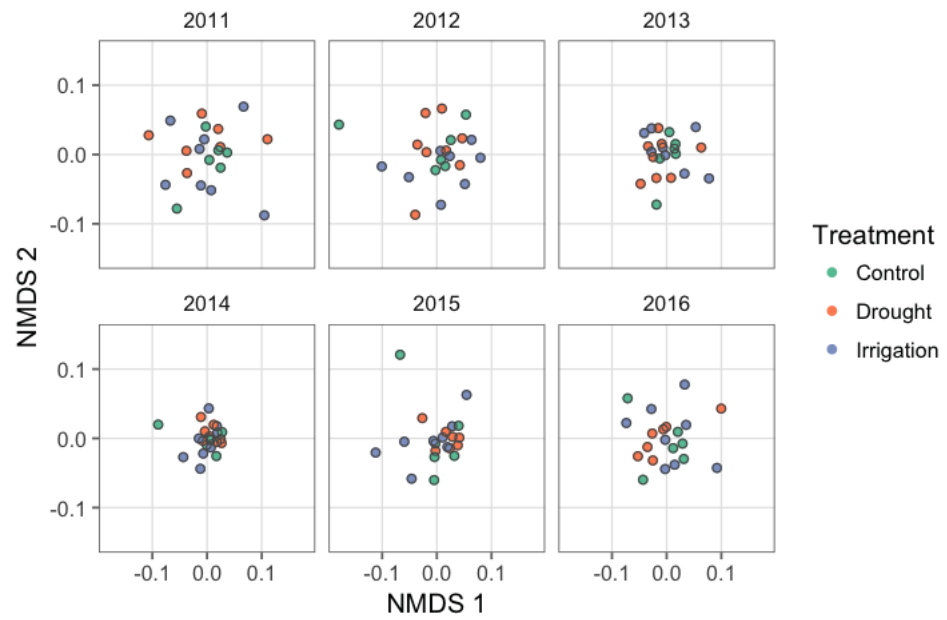


Figure 4. Nonmetric multidimensional scaling scores representing plant communities in each plot, colored by treatment.

360 References

- 361 Adler, P. B., Dalgleish, H. J., and Ellner, S. P. (2012). Forecasting plant community impacts of climate
362 variability and change: when do competitive interactions matter? *Journal of Ecology*, 100:478–487.
- 363 Avolio, M. L., Pierre, K. J. L., Houseman, G. R., Koerner, S. E., Grman, E., Isbell, F., Johnson, D. S.,
364 and Wilcox, K. R. (2015). A framework for quantifying the magnitude and variability of community
365 responses to global change drivers. *Ecosphere*, 6(12):1–14.
- 366 Bates, D., Maechler, M., Bolker, B., and Walker, S. (2015). Fitting linear mixed-effects models using
367 lme4.
- 368 Bazzaz, F. (1979). The Physiological Ecology of Plant Succession. *Annual Review of Ecology and*
369 *Systematics*, 10:351–371.
- 370 Blaisdell, J. P. (1958). Seasonal development and yield of native plants on the upper snake river plains
371 and their relation to certain climate factors. *United States Department of Agriculture Technical Bulletin*
372 *No. 1190*.
- 373 Byrne, K. M., Lauenroth, W. K., Adler, P. B., and Byrne, C. M. (2011). Estimating Aboveground Net
374 Primary Production in Grasslands: A Comparison of Nondestructive Methods. *Rangeland Ecology and*
375 *Management*, 64(5):498–505.
- 376 Dalgleish, H. J., Koons, D. N., Hooten, M. B., Moffet, C. A., and Adler, P. B. (2011). Climate influences
377 the demography of three dominant sagebrush steppe plants. *Ecology*, 92(1):75–85.
- 378 De Boeck, H. J., Dreesen, F. E., Janssens, I. A., and Nijs, I. (2011). Whole-system responses of
379 experimental plant communities to climate extremes imposed in different seasons. *New Phytologist*,
380 189(3):806–817.
- 381 Epstein, H. E., Lauenroth, W. K., and Burke, I. C. (1997). Effects of temperature and soil texture on
382 ANPP in the U.S. Great plains. *Ecology*, 78(8):2628–2631.
- 383 Franks, S. J. (2011). Plasticity and evolution in drought avoidance and escape in the annual plant *Brassica*
384 *rapa*. *New Phytologist*, 190(1):249–257.
- 385 Gelman, A. and Hill, J. (2009). *Data analysis using regression and multilevel/hierarchical models*.
386 Cambridge University Press, Cambridge.
- 387 Gherardi, L. A. and Sala, O. E. (2013). Automated rainfall manipulation system: a reliable and inexpensive
388 tool for ecologists. *Ecosphere*, 4(2):1–10.
- 389 Gherardi, L. A. and Sala, O. E. (2015a). Enhanced interannual precipitation variability increases
390 plant functional diversity that in turn ameliorates negative impact on productivity. *Ecology Letters*,
391 18(12):1293–1300.
- 392 Gherardi, L. A. and Sala, O. E. (2015b). Enhanced precipitation variability decreases grass- and increases
393 shrub-productivity. *Proceedings of the National Academy of Sciences*, 112(41):12735–12740.
- 394 Hill, R. R. (1920). Charting Quadrats with a Pantograph. *Ecology*, 1(4):270–273.
- 395 Hoover, D. L., Knapp, A. K., and Smith, M. D. (2014). Resistance and resilience of a grassland ecosystem
396 to climate extremes. *Ecology*, 95(9):2646–2656.
- 397 Hsu, J. S., Powell, J., and Adler, P. B. (2012). Sensitivity of mean annual primary production to
398 precipitation. *Global Change Biology*, 18(7):2246–2255.
- 399 Knapp, A. K., Avolio, M. L., Beier, C., Carroll, C. J. W., Collins, S. L., Dukes, J. S., Fraser, L. H., Griffin-
400 Nolan, R. J., Hoover, D. L., Jentsch, A., Loik, M. E., Phillips, R. P., Post, A. K., Sala, O. E., Slette, I. J.,
401 Yahdjian, L., and Smith, M. D. (2017). Pushing precipitation to the extremes in distributed experiments:
402 recommendations for simulating wet and dry years. *Global Change Biology*, 23(5):1774–1782.
- 403 Knapp, A. K., Briggs, J. M., and Smith, M. D. (2012). Community stability does not preclude ecosystem
404 sensitivity to chronic resource alteration. *Functional Ecology*, 26(6):1231–1233.
- 405 Kulmatiski, A., Adler, P. B., Stark, J. M., and Tredennick, A. T. (2017). Water and nitrogen uptake are
406 better associated with resource availability than root biomass. *Ecosphere*, 8(3).
- 407 LeBauer, D. S. and Treseder, K. K. (2008). Nitrogen limitation of net primary productivity in terrestrial
408 ecosystems is globally distributed. *Ecology*, 89(2):371–379.
- 409 Lemoine, N. P., Sheffield, J., Dukes, J. S., Knapp, A. K., and Smith, M. D. (2016). Terrestrial Precipitation
410 Analysis (TPA): A resource for characterizing long-term precipitation regimes and extremes. *Methods*
411 *in Ecology and Evolution*, 7(11):1396–1401.
- 412 Oksanen, J. (2016). *Vegan: ecological diversity*.
- 413 R Core Team (2016). *R: A Language and Environment for Statistical Computing*. Vienna, Austria.

- 414 Seger, J. (1987). What is bet-hedging? In Harvey, P. and Partridge, L., editors, *Oxford surveys in*
415 *evolutionary biology*, pages 182–211. Oxford University Press, Oxford.
- 416 Smith, M. (2011). An ecological perspective on extreme climatic events: A synthetic definition and
417 framework to guide future research. *Journal of Ecology*, 99(3):656–663.
- 418 Smith, M. D., Knapp, A. K., and Collins, S. L. (2009). A framework for assessing ecosystem dynamics in
419 response to chronic resource alterations induced by global change. *Ecology*, 90(12):3279–3289.
- 420 Stan Development Team (2016a). Rstan: the R interface to Stan, Version 2.14.1.
- 421 Stan Development Team (2016b). Stan: A C++ Library for Probability and Sampling, Version 2.14.1.
- 422 Wilcox, K. R., Blair, J. M., Smith, M. D., and Knapp, A. K. (2016). Does ecosystem sensitivity to
423 precipitation at the site-level conform to regional-scale predictions? *Ecology*, 97(3):561–568.

Appendix 1

A.T. Tredennick, A.R. Kleinhesselink, B. Taylor & P.B. Adler

“Consistent ecosystem functional response across precipitation extremes in a sagebrush steppe”

PeerJ

Section A1.1 Estimating ANPP

We used a radiometer to nondestructively estimate aboveground net primary productivity. Our approach relies on relating greenness in a plot to aboveground biomass. In each year we recorded ground reflectances at four bands, two associated with the red spectrum and two associated with the near-infrared spectrum (Table A1-1). We took four readings per plot that were averaged for each band. Bands 1 and 3 correspond to wavelengths collected by the MODIS satellite and bands 2 and 4 correspond to wavelengths collected by the AVHRR satellite.

Table A1-1 Radiometer specifications.

Band number	Spectrum name	Center wavelength	Corresponding satellite
1	red	626 nm	AVHRR
2	red	652 nm	MODIS
3	near-infrared	875 nm	AVHRR
4	near-infrared	859 nm	MODIS

Using the RED and NIR reflectance values, we calculate the normalized difference vegetation index (NDVI) for each plot based on both AVHRR- and MODIS-based wavelengths. We calculated NDVI as:

$$\text{NDVI}_{\text{AVHRR}} = \frac{b_3 - b_1}{b_3 + b_1} \quad (1)$$

$$\text{NDVI}_{\text{MODIS}} = \frac{b_4 - b_2}{b_4 + b_2} \quad (2)$$

where b_x refers to band x ($x = 1,2,3,4$) in Table A1-1.

To convert plot NDVI to biomass, we regressed known biomass values from calibration plots against NDVI calculate for those plots. Calibration plots were located near our experiment plots, and each year we located a new set of 10 plots in which we clipped all aboveground biomass, dried it to a constant weight at 60° C, and the weighed. We used these biomass values to estimate regression parameters for both AVHRR- and MODIS-based NDVI. We assessed model fit using

17 R^2 and, for each year, we used the regression parameters associated with the best fit model to
 18 estimate biomass in the experimental plots based on their NDVI values (Table A1-2). R code for
 19 this procedure is in the file “calibrate_radiometer_by_year.R” in the supplemental code set.

Table A1-2 Details of regression models used to estimate biomass each year.

Year	Intercept	NDVI Slope	R^2	Min(biomass)	Max(biomass)	Algorithm	NA
2012	9.03	144.23	0.59	8.57	41.42	15	MODIS
2013	1.44	111.39	0.39	8.63	77.62	15	MODIS
2014	16.31	222.38	0.63	14.61	62.30	15	MODIS
2015	-8.89	210.31	0.21	44.72	129.03	12	AVHRR
2016	14.15	493.85	0.72	50.16	163.70	16	MODIS
2017	21.67	205.64	0.57			39	MODIS

Appendix 2

A.T. Tredennick, A.R. Kleinhesselink, B. Taylor & P.B. Adler

“Consistent ecosystem functional response across precipitation extremes in a sagebrush steppe”

PeerJ

Section A2.1 Random Slopes, Random Intercepts Model

Section A2.1.1 Model Description

Our hierarchical Bayesian model allows us to test for differences among treatments in the relationship between ANPP and soil moisture, and allowed us to account for the non-independence of observations through time within a plot. Treatment differences are modeled as fixed effects, which are modified by plot-level random effects. In what follows, \mathbf{X} is the fixed effects design matrix including:

1. a column of 1s for intercepts
2. a column of continuous values for the scaled volumetric water content for each observation
3. a column of 0s or 1s indicating whether the observation is from a drought treatment
4. a column of 0s or 1s indicating whether the observation is from an irrigation treatment
5. a column of continuous values for the interaction between scaled volumetric water content and the drought treatment indicator (column 2)
6. a column of continuous values for the interaction between scaled volumetric water content and the irrigation treatment indicator (column 3)

The first seven rows of the fixed effects design matrix (six control plots and one drought plot) is as follows:

##	Int	WVC	Drought	Irrig	Drought:WVC	Irrig:WVC
## 1	1	-1.543513	0	0	0.000000	0
## 2	1	-1.543513	0	0	0.000000	0
## 3	1	-1.543513	0	0	0.000000	0
## 4	1	-1.543513	0	0	0.000000	0
## 5	1	-1.543513	0	0	0.000000	0
## 6	1	-1.543513	0	0	0.000000	0
## 7	1	-2.063694	1	0	-2.063694	0

Note that within a year, all plots within a treatment share the same value of volumetric water content. This is because we could not monitor soil moisture in each plot, and instead used sparse observations to model average soil moisture in each treatment in each year (see main text). Using this design matrix, we can estimate six fixed effects (β s):

1. the intercept of the soil moisture-ANPP relationship for control plots
2. the slope of the soil moisture-ANPP relationship for control plots
3. the intercept offset for drought plots
4. the intercept offset for irrigation plots
5. the slope offset for drought plots
6. the slope offset for irrigation plots

We are particularly interested in the slope offsets, because these allow us to test whether the slopes for drought or irrigation are different from the control slope. If the slope offset is different from zero, this indicates the slopes are different. We assess whether the slope offsets are different from zero by calculating the probability that the posterior distribution is less or greater than zero (one-tailed tests). If the probability is greater than 0.95, then there is strong evidence that the slope offset is different from zero, and thus different from the control treatment slope.

To account for the fact that observations within plots through time are not independent, we include random effects that modify the fixed effects in each plot. We model these random effects (γ s) as offsets drawn from a multivariate normal distribution with mean 0 and a variance-covariance matrix (Σ) that includes a covariance between the intercept and slope offsets. We implement this random effects structure by including a random effects design matrix (\mathbf{Z}) with a column of 1s for intercept offsets and a column of continuous values for the volumetric water content for each observation.

Lastly, to account for unknown variation across years, we include random year effects. These year effects (η s) act as offsets on the intercept.

Putting it all together, our model is defined mathematically as follows, where i denotes observation, j denotes plot, and t denotes year. We assume the observations are conditionally Gaussian,

$$\mathbf{y} \sim \text{Normal}(\boldsymbol{\mu}, \sigma^2), \quad (\text{A2.1})$$

where $\boldsymbol{\mu}$ is the deterministic expectation from the regression model,

$$\mu_i = \beta \mathbf{x}_i + \gamma_{j(i)} \mathbf{z}_i + \eta_t. \quad (\text{A2.2})$$

All fixed effect β s were drawn from normally distributed priors with mean 0 and standard deviation 5: $\beta \sim \text{Normal}(0, 5)$. γ random effects were drawn from a multivariate prior centered on zero with a shared variance covariance matrix:

$$\boldsymbol{\gamma} \sim \text{MVN}(0, \boldsymbol{\Sigma}), \quad (\text{A2.3})$$

$$\boldsymbol{\Sigma} = \sigma_{plt}^2 \mathbf{R}, \quad (\text{A2.4})$$

$$\sigma_{plt} \sim \text{Cauchy}(0, 2.5), \quad (\text{A2.5})$$

$$\mathbf{R} \sim \text{LKJ}(2.0) \quad (\text{A2.6})$$

61 The random year effects ($\boldsymbol{\eta}$) are modeled as intercept offsets centered on zero with a shared
 62 variance (σ_{yr}): $\boldsymbol{\gamma} \sim \text{Normal}(0, \sigma_{yr})$.

63 The Bayesian posterior distribution of our model can be expressed as:

$$[\boldsymbol{\beta}, \boldsymbol{\gamma}, \boldsymbol{\eta}, \sigma_{yr}, \sigma_{plt}, \mathbf{R}, \sigma | \mathbf{y}] \propto \left(\prod_{i=1}^n [y_i | \boldsymbol{\beta}, \boldsymbol{\gamma}, \boldsymbol{\eta}, \sigma] \right) \left(\prod_{j=1}^J [\gamma_j | \sigma_{plt}, \mathbf{R}] \right) \quad (\text{A2.7})$$

$$\times \left(\prod_{t=1}^T [\eta_t | \sigma_{yr}] \right) [\boldsymbol{\beta}] [\sigma_{plt}] [\mathbf{R}] [\sigma_{yr}] [\sigma] \quad (\text{A2.8})$$

64 We fit the model using MCMC as implemented in the software Stan (Stan Development Team 2016).
 65 Our Stan code is below. All code necessary to reproduce our results has been archived on Figshare
 66 ([link here](#)) and released on GitHub (https://github.com/atredennick/usses_water/releases/v0.1).

```

data {
  int<lower=0> Npreds;           # number of covariates, including intercept
  int<lower=0> Npreds2;          # number of random effect covariates
  int<lower=0> Nplots;           # number of plots
  int<lower=0> Ntreats;          # number of treatments
  int<lower=0> Nobs;             # number of observations
  int<lower=0> Nyears;           # number of years
  vector[Nobs] y;               # vector of observations
  row_vector[Npreds] x[Nobs];   # design matrix for fixed effects
  row_vector[Npreds2] z[Nobs];  # simple design matrix for random effects
  int plot_id[Nobs];            # vector of plot ids
  int treat_id[Nobs];           # vector of treatment ids
  int year_id[Nobs];            # vector of year ids
}

parameters {
  vector[Npreds] beta;          # overall coefficients
  vector[Nyears] year_off;      # vector of year effects
  cholesky_factor_corr[Npreds2] L_u; # cholesky factor of plot random effect corr matrix
  vector[Npreds2] beta_plot[Nplots]; # plot level random effects
  vector<lower=0>[Npreds2] sigma_u; # plot random effect std. dev.
  real<lower=0> sd_y;            # treatment-level observation std. dev.
  real<lower=0> sigma_year;      # year std. dev. hyperprior
}

transformed parameters {
  vector[Nobs] yhat;            # vector of expected values
  vector[Npreds2] u[Nplots];    # transformed plot random effects
  matrix[Npreds2,Npreds2] Sigma_u; # plot ranef cov matrix

  Sigma_u = diag_pre_multiply(sigma_u, L_u); # plot-level covariance matrix
  for(j in 1:Nplots)
    u[j] = Sigma_u * beta_plot[j]; # plot random intercepts and slopes

  # regression model for expected values (one for each plot-year)
  for (i in 1:Nobs)
    yhat[i] = x[i]*beta + z[i]*u[plot_id[i]] + year_off[year_id[i]];

```

```

}

model {
  ##### PRIORS
  sigma_u ~ cauchy(0,2.5)
  sigma_year ~ cauchy(0,2.5)
  year_off ~ normal(0,sigma_year); # priors on year effects, shared variance
  beta ~ normal(0,5);              # priors on treatment coefficients
  L_u ~ lkj_corr_cholesky(2.0);    # prior on the cholesky factor which controls the
                                   # correlation between plot level treatment effects

  for(i in 1:Nplots)
    beta_plot[i] ~ normal(0,1); # plot-level coefficients for intercept and slope

  ##### LIKELIHOOD
  for(i in 1:Nobs)
    y[i] ~ normal(yhat[i], sd_y); # observations vary normally around expected values
}

generated quantities{
  corr_matrix[Npreds2] R = multiply_lower_tri_self_transpose(L_u);
  cov_matrix[Npreds2] V = quad_form_diag(R,sigma_u);
}

```

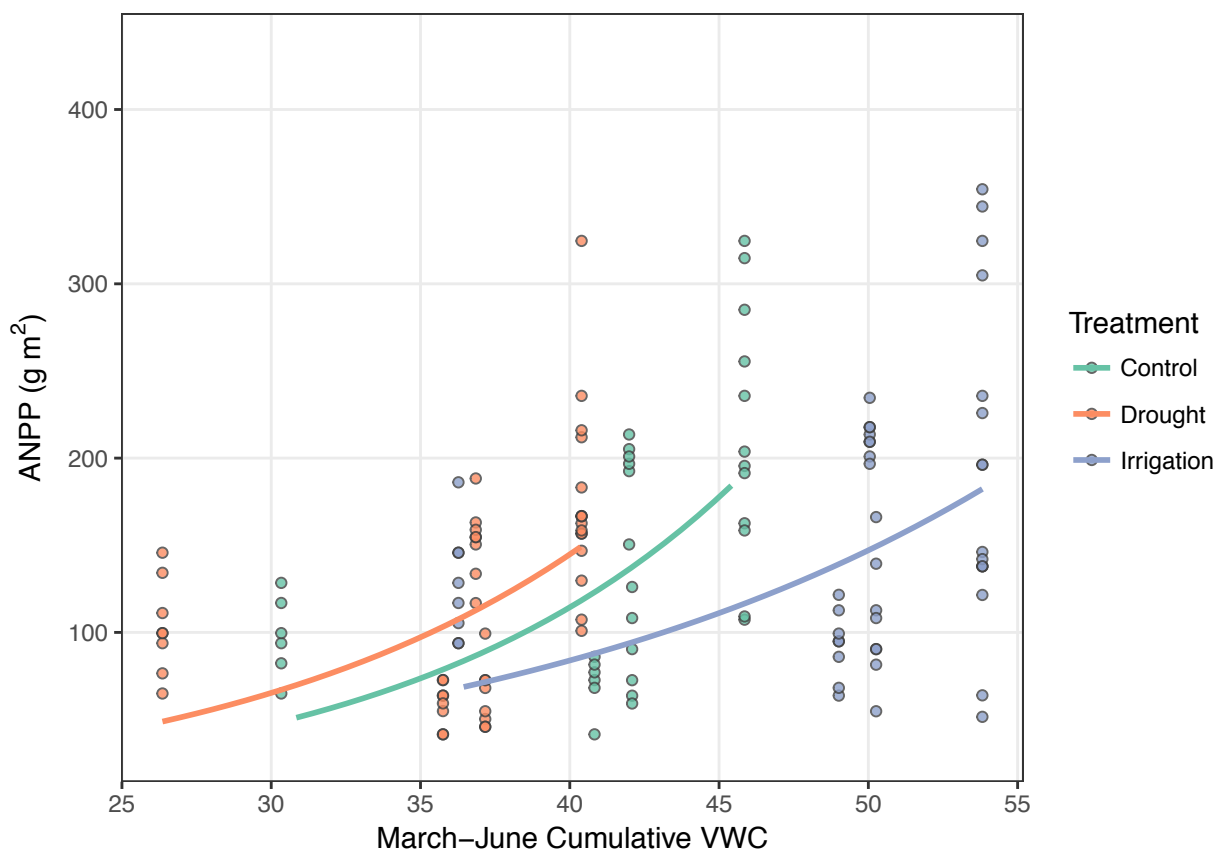


Figure A2-1 Scatterplot, on the arithmetic scale, of the data and model estimates shown as solid lines. Model estimates come from treatment level coefficients (colored lines).

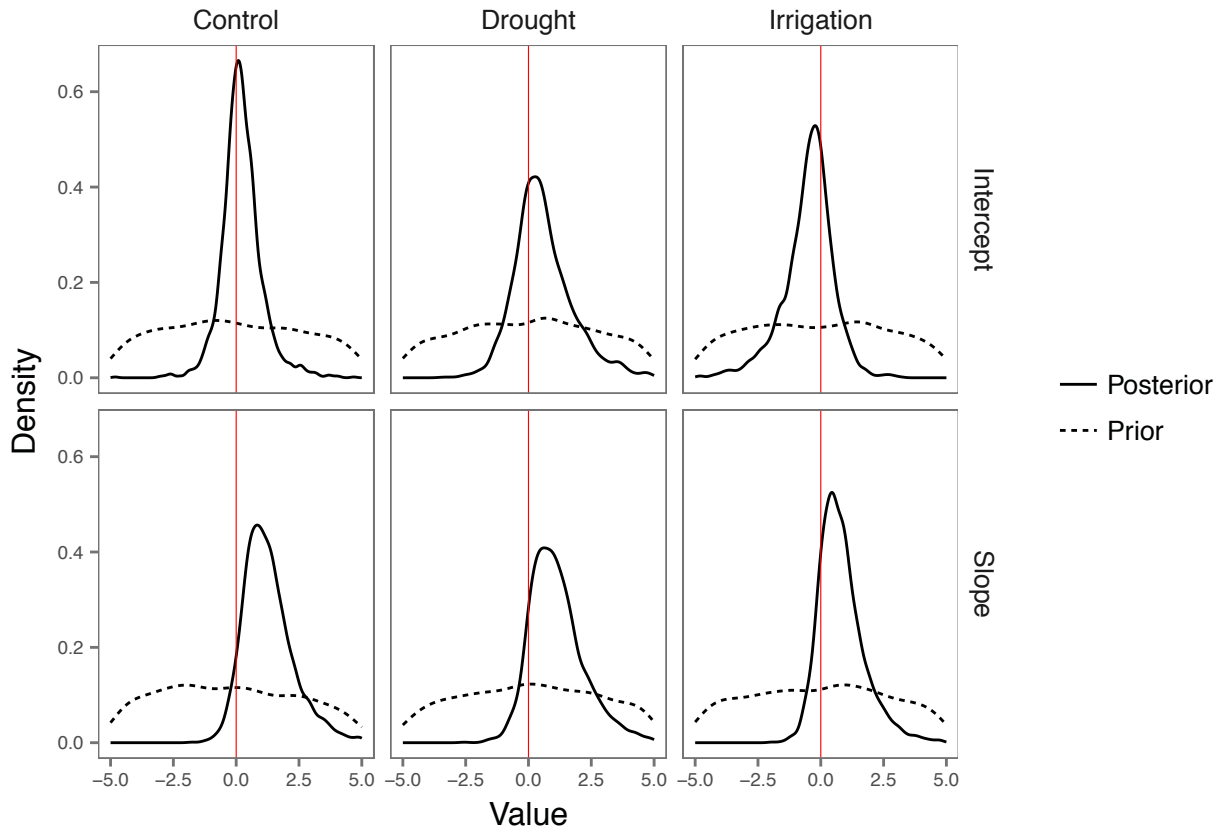


Figure A2-2 Prior (dashed lines) and posterior (solid line) distributions of intercepts and slopes for each treatment. The slope represents the main effect of soil moisture on $\log(\text{ANPP})$. The red line marks 0. Shrinkage of the posterior distribution and/or changes in the mean indicate the data informed model parameters beyond the information contained in the prior for all coefficients.

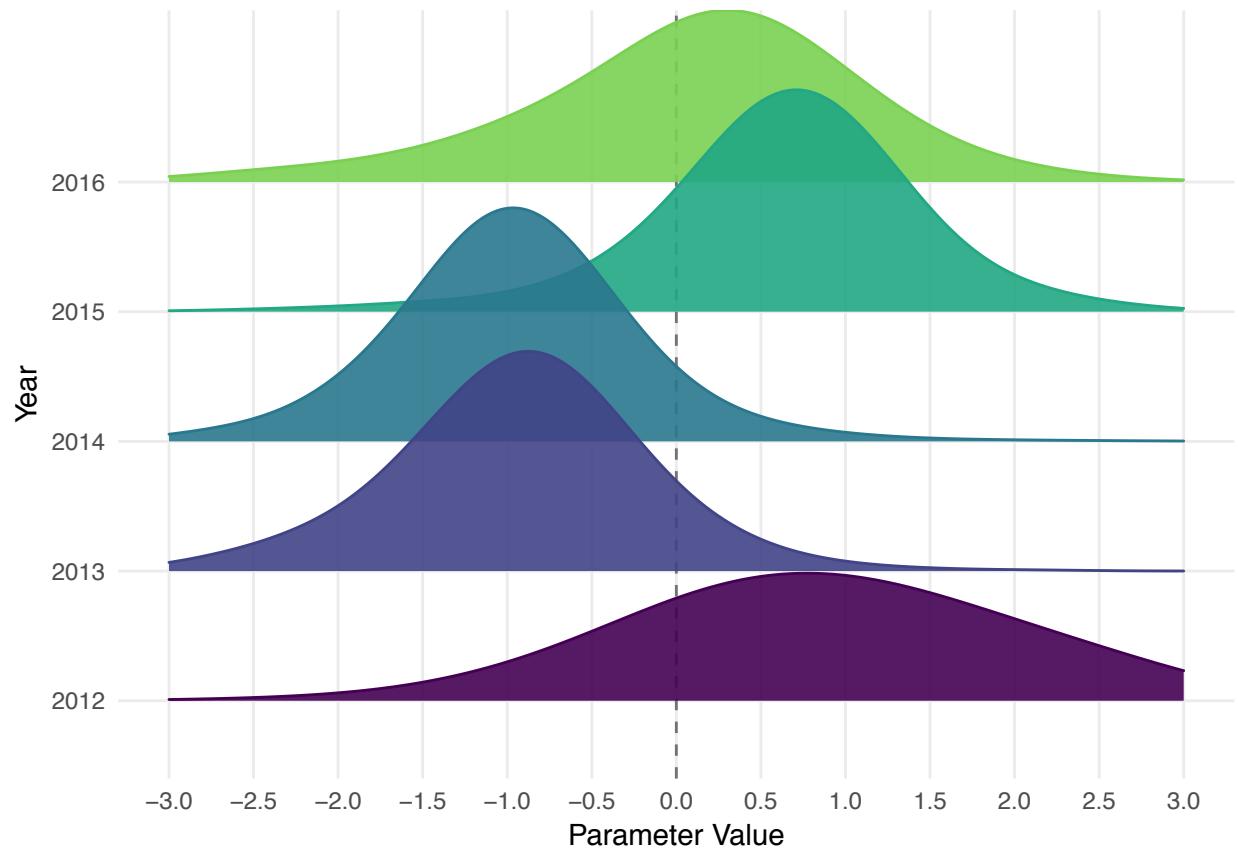


Figure A2-3 Posterior distributions of random year effects (intercept offsets). Kernel bandwidths of posterior densities were adjusted by a factor of 5 to smooth the density curves for visual clarity.

69 **References**

- 70 Stan Development Team. 2016. Stan: A C++ Library for Probability and Sampling, Version 2.14.1.

Appendix 3

A.T. Tredennick, A.R. Kleinhesselink, B. Taylor & P.B. Adler

"Consistent ecosystem functional response across precipitation extremes in a sagebrush steppe"

PeerJ

Section A3.1 Characterizing Extreme Precipitation Amounts

Following the proposed methods of Lemoine et al. (2016), we calculated quantiles from the empirical distribution of growing season precipitation at Dubios, ID. We chose the 1% quantile to be indicative of extreme dry conditions (drought) and the 99% quantile to be indicative of extreme wet conditions (irrigation). The data consist of 91 yearly records, which we assume are approximately normally distributed. The R code below shows our procedure, and Fig. A3-1 shows the results.

```
library(ggplot2)
weather      <- read.csv("../data/weather/ClimateIPM.csv")
mean_ppt     <- mean(weather$ppt1)
quants_ppt   <- quantile(weather$ppt1, probs = c(0.01, 0.99))
quants_ppt[1]/mean_ppt*100 # percent of mean ppt for drought
```

```
##          1%
## 46.96351
```

```
quants_ppt[2]/mean_ppt*100 # percent of mean ppt for irrigation
```

```
##          99%
## 177.727
```

```
ggplot(weather, aes(x=ppt1))+
  geom_histogram(bins=20, color="dodgerblue", fill="dodgerblue", aes(y=..density..))+
  geom_line(stat="density", color="blue")+
  geom_vline(aes(xintercept=quants_ppt[1]), linetype=2)+
  geom_vline(aes(xintercept=quants_ppt[2]), linetype=2)+
  ylab("Density")+
  xlab("Growing Season Precipitation (mm)")+
  theme_bw()+
  theme(panel.grid.minor = element_blank())
```

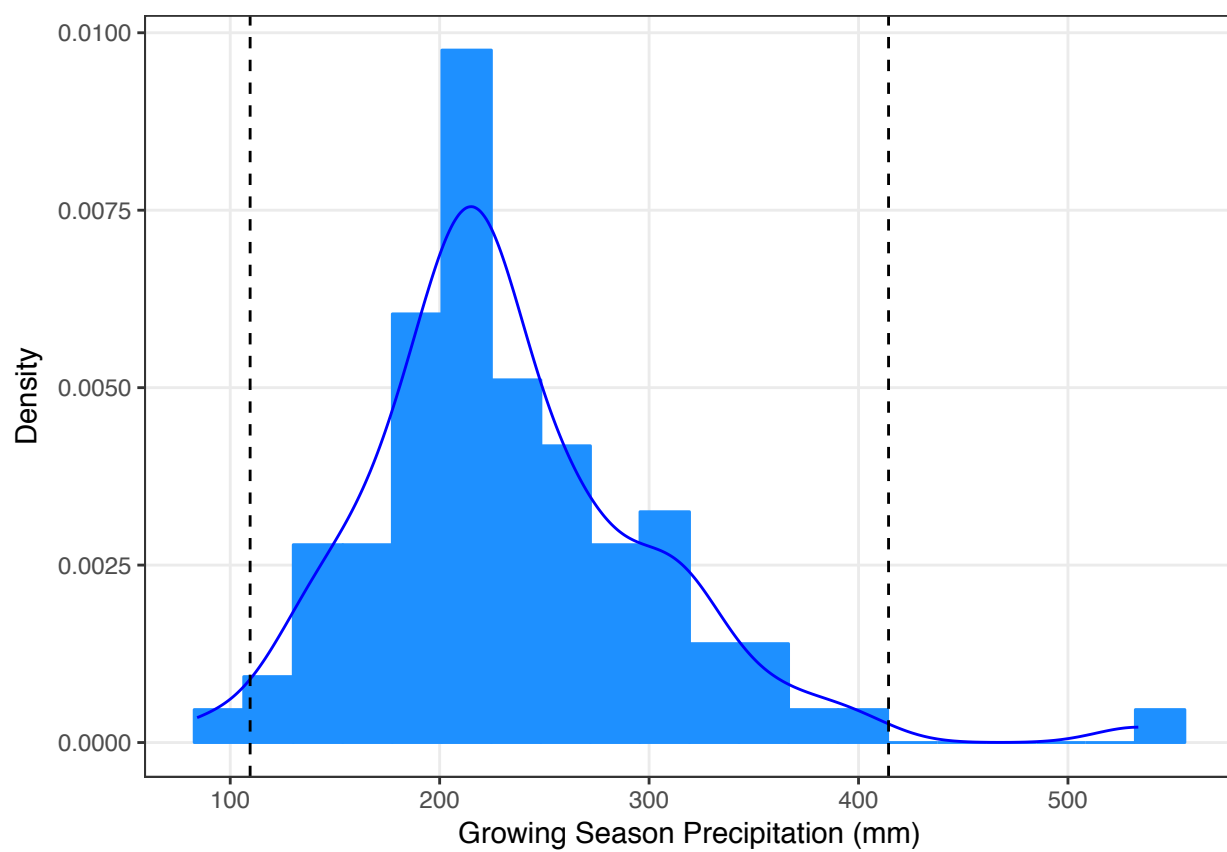


Figure A3-1 Density of the empirical distribution of growing season precipitation at Dubois, ID. Dashed vertical lines show the 1% and 99% quantiles, assuming a normal distribution.

16 **References**

- 17 Lemoine, N. P., J. Sheffield, J. S. Dukes, A. K. Knapp, and M. D. Smith. 2016. Terrestrial
18 Precipitation Analysis (TPA): A resource for characterizing long-term precipitation regimes and
19 extremes. *Methods in Ecology and Evolution* 7:1396–1401.